

# ATLAS Tracking and Vertexing Performance

Ben Cooper for the ATLAS Collaboration

Queen Mary University of London, Mile End Road, London, UK

DOI: <http://dx.doi.org/10.5689/UA-PROC-2010-09/45>

In these proceedings are presented a selection of studies which investigate the charged particle tracking and vertexing performance of the ATLAS Inner Detector. Tracking at ATLAS is found to be performing very well, and detailed comparison to the expectations from detector simulated Monte Carlo collision events demonstrate the high degree of understanding of the tracking that has already been achieved.

## 1 Introduction

The ATLAS detector [1] is a large multi-purpose particle physics detector that is designed to analyse the high energy proton-proton collisions produced by the Large Hadron Collider (LHC) at CERN. ATLAS comprises four major subsystems, the Inner Detector (ID), Electromagnetic Calorimeter, Hadronic Calorimeter and Muon Spectrometer. The ID is the innermost detector subsystem, contained within a 2T solenoidal magnetic field which has field lines parallel to the beamline. The primary role of the ID is to accurately and efficiently reconstruct the helical trajectory of charged particles emerging from the interaction point. Figure 1 shows a 3-D view of the ATLAS ID. Visible are the three subdetectors of the ID; the Pixel detector, Semiconductor

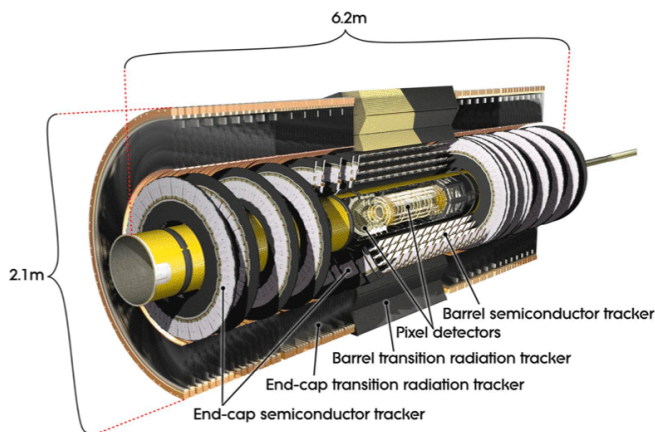


Figure 1: The ATLAS Inner Detector.

Tracker (SCT) and Transition Radiation Tracker (TRT). Table 1 reports the type of each subdetector, the number of modules and their resolutions [1].

Subdetector	Pixel		SCT		TRT	
	Barrel	Endcap	Barrel	Endcap	Barrel	Endcap
No. of Layers/Disks	3	$2 \times 3$	4	$2 \times 9$	3	$2 \times 40$
No. of Modules	1456	$2 \times 144$	2112	$2 \times 988$	96	$2 \times 40$
Detector Technology	silicon pixels		silicon strips		gaseous straw tubes	
Resolutions	$10 \mu\text{m} (R\phi)$		$17 \mu\text{m} (R\phi)$		$130 \mu\text{m} (R\phi)$	
	$115 \mu\text{m} (z/R)$		$580 \mu\text{m} (z/R)$			

Table 1: Components of the ATLAS Inner Detector.

## 2 Inner Detector Alignment

At high track  $p_T$  ( $p_T > 15$  GeV), the tracking performance is determined largely by the resolution of the individual hit-on-track measurements. This in turn is limited by the quality of the *alignment* of the ID modules; the accuracy with which the position and orientation of the ID modules is known. In order not to degrade track parameter resolutions by more than 20% at infinite momenta it is estimated that alignment to an accuracy of  $10 \mu\text{m}$  in the  $R\phi$  direction is required [2].

The alignment of the ATLAS ID has thus far been carried out using track-based alignment approaches [3]. Recently, the alignment has been updated to use tracks from proton-proton collisions at a centre-of-mass energy of 7 TeV, enabling the alignment to be carried out with a much larger number of high momenta tracks than before. Figure 2 shows the track-hit  $R\phi$  residual distributions for all modules in the Pixel, SCT and TRT barrels. The tracks are from events taken using a minimum bias trigger, requiring track  $p_T > 2$  GeV, and are compared to tracks in a Monte Carlo simulation of minimum bias events. One can see that in all cases the width of the residual distributions in the data are close to or in agreement with that observed in the simulation, indicating the high precision of the alignment that has now been achieved. Residual distributions of modules in the endcaps show a similar level of performance.

## 3 ID Reconstruction of Low Mass Resonance Decays

Charged particle tracks in the ID can be used to reconstruct  $K_S^0 \rightarrow \pi^+\pi^-$  and  $J/\psi \rightarrow \mu^+\mu^-$  decays which occur within the ID volume. These analyses are fully described in [4, 5]. Figure 3 shows the reconstructed  $K_S^0$  mass compared with the expectation from signal and background simulation. The mass distribution is shown separately for the cases where the pion tracks are restricted to the barrel region,  $|\eta| < 1.2$ , and the endcap region,  $|\eta| > 1.2$ . For the barrel region, the  $K_S^0$  mass peak is reconstructed in the data at  $497.427 \pm 0.006$  MeV (statistical error only), which agrees very well with the PDG value [6] ( $497.614 \pm 0.024$  MeV), and also the value from simulation ( $497.329 \pm 0.006$  MeV). The fitted Gaussian width in the data (5.60 MeV) is also in good agreement with the simulation (5.42 MeV). A similar level of agreement between the data, PDG value and simulation in both mean and width is observed in the endcaps.

Figure 4 (left-side) shows the ID reconstructed  $J/\psi$  mass, with an unbinned maximum likelihood fit to all muon pairs in the range  $2 < m_{\mu\mu} < 4$  GeV, compared with the prediction from simulated prompt  $J/\psi$  Monte Carlo (where the simulation is normalised to the signal peak in the data). Figure 4 (right-side) shows the mean of the fitted signal mass peak as a function of the pseudo-rapidity of the furthest forward muon, compared with the expectation

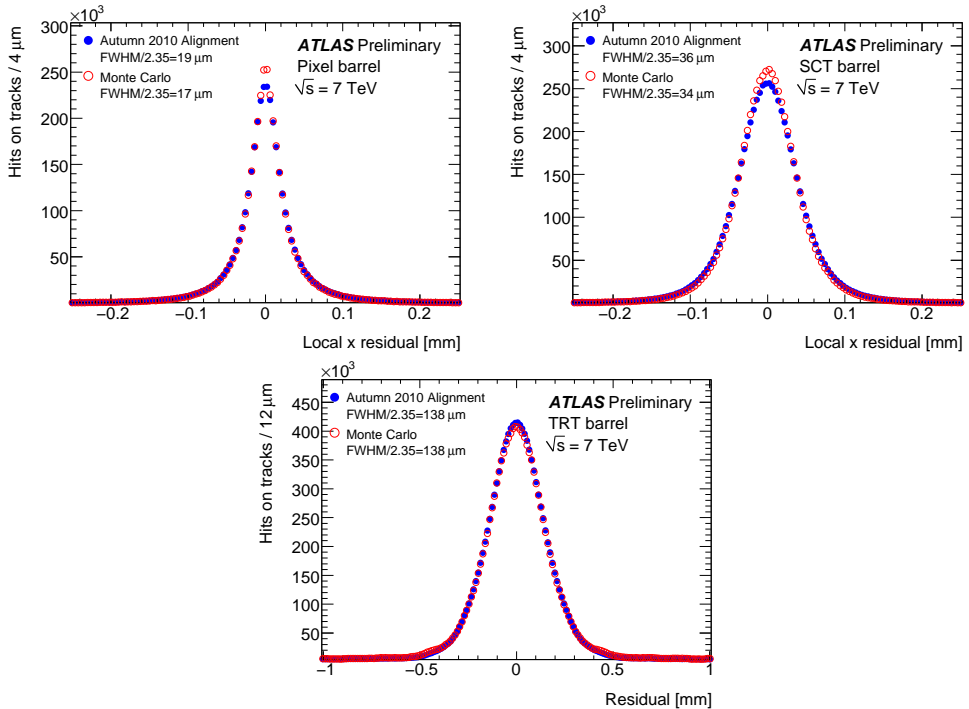


Figure 2: Hit-on-track  $R\phi$  residual distributions for barrel modules in the Pixel, SCT and TRT detectors.

from the simulation, and the PDG value [6]. No deviation of the mean mass from the PDG value larger than  $0.2 \pm 0.1\%$  is observed. The width of the signal peak is also observed to be in good agreement with the simulation expectation.

These  $K_S^0$  and  $J/\psi$  studies provide an excellent validation of the momentum scale at low track  $p_T$  ( $p_T < 5$  GeV), and demonstrate the quality of the ID material description and alignment that has already been achieved.

## 4 Impact Parameter and Primary Vertex Reconstruction

A primary vertex reconstruction algorithm is used to determine the position of the primary interaction vertex and of possible additional “pile-up” interactions taking place in the same bunch crossing. An iterative vertex finding algorithm [7] is used, where iteration-by-iteration outlier tracks which are incompatible with the present vertex position are down-weighted, and eventually may be used to seed a new vertex. Figure 5 shows the primary vertex resolution as a function of the number of tracks used in the vertex fit. This is determined using a data-driven method, in which single vertices in the data are split into two and refitted, with the width of the resultant vertex separation distribution giving the single vertex resolution. The single vertex resolution is  $\sim 30 \mu\text{m}$  in the plane transverse to the beamline, and  $\sim 50 \mu\text{m}$  in the direction along the beamline, for vertices with seventy associated tracks.

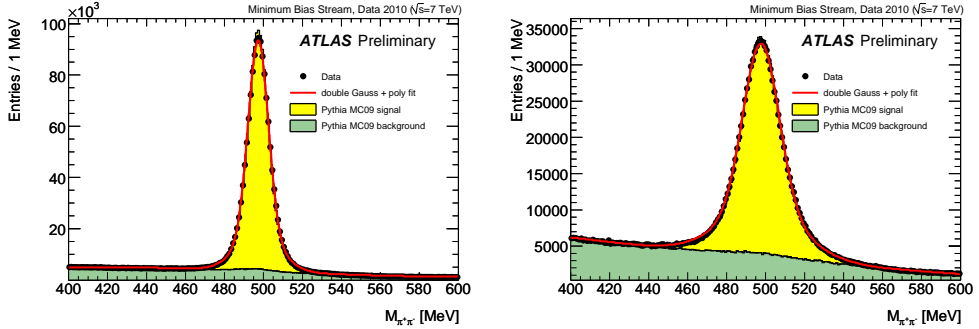


Figure 3: Invariant mass distribution of  $K_S^0 \rightarrow \pi^+\pi^-$  decays reconstructed in the ID, where the pion tracks are restricted to the barrel region  $|\eta| < 1.2$  (left), and the endcap region  $|\eta| > 1.2$  (right).

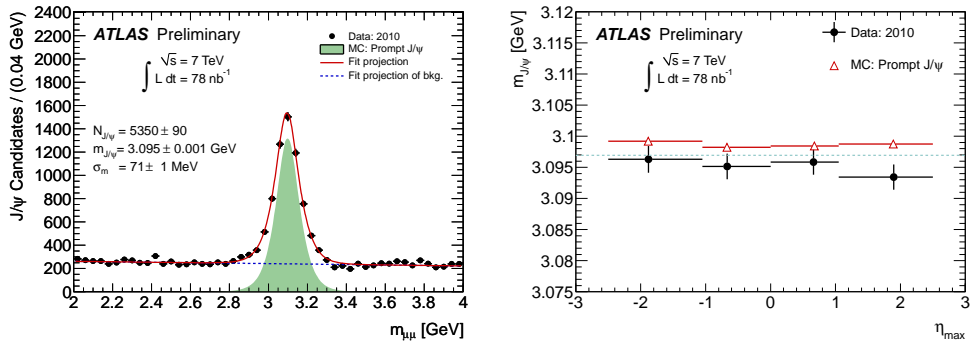


Figure 4: Invariant mass distribution of  $J/\psi \rightarrow \mu^+\mu^-$  decays reconstructed in the ID (left), and the mean of the fitted signal  $J/\psi$  mass peak as a function of pseudo-rapidity of the furthest forward muon (right).

Figure 6 (left-side) shows the impact parameter  $d_0$  (distance of closest approach to the primary vertex in the transverse plane) distribution of tracks in a data sample collected with a jet trigger, compared to the expectation from a dijet Monte Carlo simulation. The width of this distribution is a convolution of the  $d_0$  resolution ( $\sigma_{d_0}$ ) and the primary vertex resolution in the transverse plane ( $\sigma_{PV}$ ). An iterative procedure is used to de-convolute  $\sigma_{d_0}$  from  $\sigma_{PV}$  in the data [8]. In Figure 6 (right-side), the resulting deconvoluted  $\sigma_{d_0}$  is plotted as a function of track  $p_T$ , and compared with the  $d_0$  resolution determined in the simulation. Excellent agreement between data and simulation is seen at low  $p_T$ , but a divergence is seen at higher  $p_T$  which is likely due to the impact of residual ID module misalignments in the data.

## 5 Tracking Efficiency

In general the ID track reconstruction efficiency at ATLAS has to be obtained from the simulation [9]. In the previous sections we have already seen examples of the high quality of the

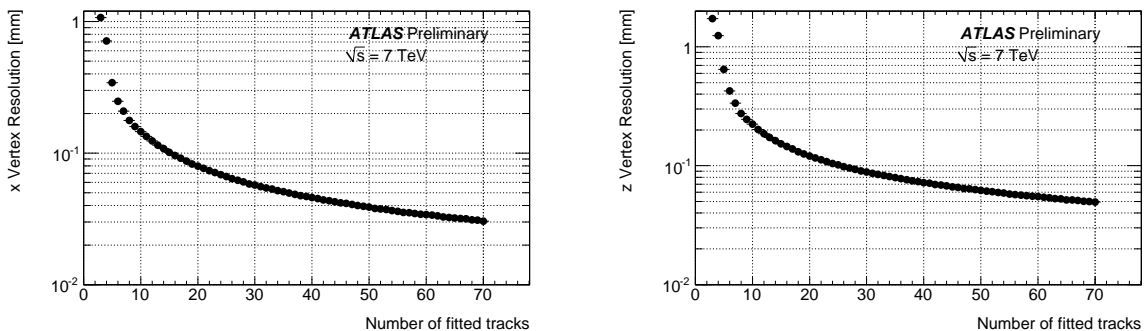


Figure 5: The single vertex resolution as a function of the number of tracks used in the vertex fit, in the plane transverse to the beamline (left), and in the direction parallel to the beamline (right).

modelling of the ID performance that is obtainable with the simulation. Figure 7 gives two further examples; on the left we see that the simulation is able to well reproduce the average number of Pixel hits on track as a function of pseudo-rapidity seen in data, and on the right, the simulation is also able to predict the relative efficiency to reconstruct a standalone track in the Pixel detector, if a track has already been found using hits in the SCT and TRT detectors [10]. The dominant uncertainty on the determination of the tracking efficiency from simulation is in the description of the material, which is currently being improved.

## 6 Conclusions

The studies presented in these proceedings demonstrate that the work undertaken over the past years in aligning the ID modules, improving the material description and optimizing the tracking algorithms has paid off, and that charged particle tracking at ATLAS is performing extremely well. They also show that the details of this tracking performance are well reproduced in the detector simulation, thus enabling the reliable use of Monte Carlo simulations to account for tracking effects in physics analyses.

## References

- [1] ATLAS Collaboration, JINST **3** (2008) S08003.
- [2] ATLAS Collaboration, CERN/LHCC/97-16/17 (1997).
- [3] ATLAS Collaboration, ATLAS-CONF-2010-067 (2010).
- [4] ATLAS Collaboration, ATLAS-CONF-2010-033 (2010).
- [5] ATLAS Collaboration, ATLAS-CONF-2010-078 (2010).
- [6] K. Nakamura et al. (Particle Data Group), J. Phys. G **37**, 075021 (2010).
- [7] ATLAS Collaboration, ATLAS-CONF-2010-069 (2010).
- [8] ATLAS Collaboration, ATLAS-CONF-2010-070 (2010).
- [9] ATLAS Collaboration, Phys. Lett. **B688** (2010) 21-42, [arXiv:1003.3124 [hep-ex]].
- [10] ATLAS Collaboration, ATLAS-CONF-2010-047 (2010).

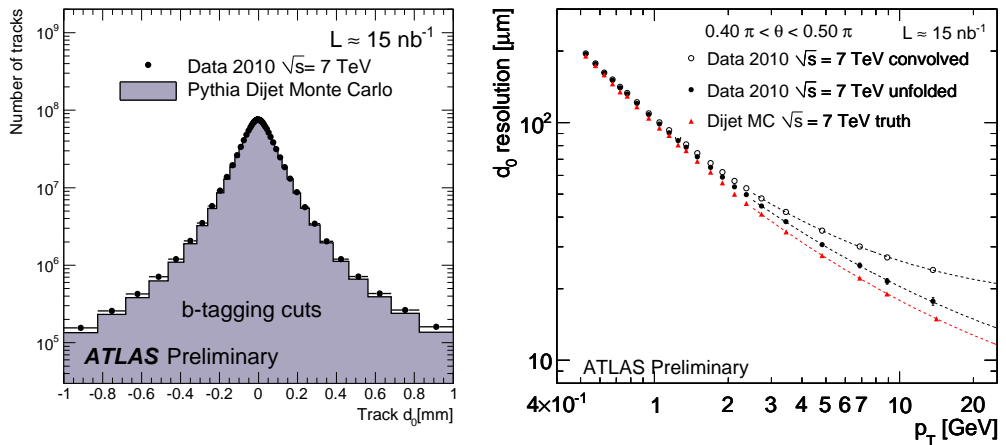


Figure 6: The distribution of transverse impact parameter  $d_0$  (left) and the deconvolved impact parameter resolution  $\sigma_{d_0}$  as a function of track  $p_T$  (right). These tracks are required to have at least seven precision (Pixel or SCT) hits, at least two Pixel hits, and  $p_T > 1 \text{ GeV}$ . In addition, one of the Pixel hits must be in the innermost layer [8].

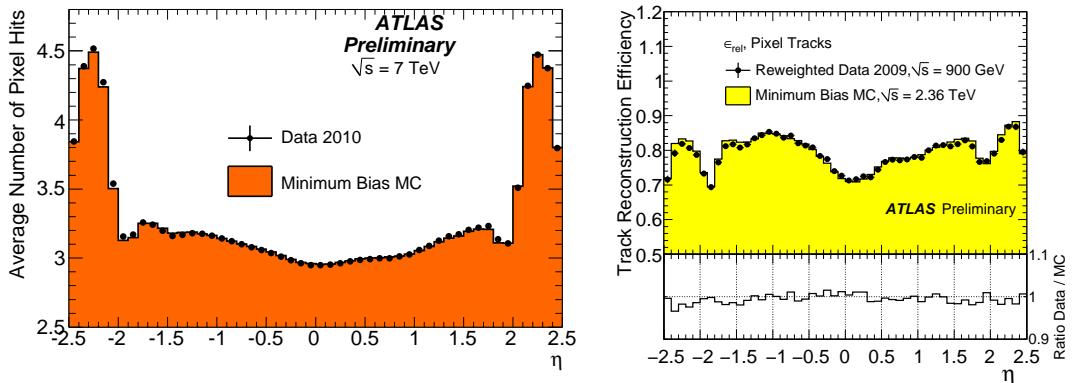


Figure 7: Average number of Pixel hits on track as a function of pseudo-rapidity (left) and relative Pixel track reconstruction efficiency (right).